

**ELECTRONIC APPENDIX TO:
ELASTIC-PLASTIC CONTACT OF A ROUGH SURFACE WITH WEIERSTRASS
PROFILE**

Yan-Fei Gao and A. F. Bower

Division of Engineering, Brown University, Providence, RI 02912, USA

Appendix A: Approximate expressions for contact response of a sinusoidal surface

In this appendix, we list the expressions that characterize the response of an elastic-perfectly plastic solid with sinusoidal roughness to indentation by a rigid flat punch. The substrate is an elastic-perfectly plastic solid with Young's modulus E , Poisson's ratio ν and yield stress \mathbf{s}_Y . The surface roughness has wavelength \mathbf{l}_n and amplitude g_n . In terms of these parameters, we define a material and geometrical parameter $\mathbf{y}_n = g_n E / [(1 - \nu^2) \mathbf{l}_n \mathbf{s}_Y]$, which characterizes the resistance of the surface to plastic flow. The solid is indented by a flat, rigid surface, under the action of a nominal pressure \bar{p}_n . The loading induces a contact width $2a_n$, pressure distribution $p_n(x)$ and mean pressure p_n^{mean} , given by functional relationships

$$\begin{aligned} 2a_n / \mathbf{l}_n &= A \left(\frac{\bar{p}_n}{\mathbf{s}_Y}, \mathbf{y}_n \right) \\ \frac{p_n(x)}{\mathbf{s}_Y} &= \Phi \left(\frac{x}{\mathbf{l}_n}, \frac{\bar{p}_n}{\mathbf{s}_Y}, \mathbf{y}_n \right) \\ \frac{p_n^{mean}}{\mathbf{s}_Y} &= \Phi^{mean} \left(\frac{\bar{p}_n}{\mathbf{s}_Y}, \mathbf{y}_n \right) \end{aligned} \quad (\text{A1})$$

We also give expressions for the pressure distribution function $q_n(p/\mathbf{s}_Y)$, which is defined so that $q_n(p/\mathbf{s}_Y)(dp/\mathbf{s}_Y)$ is the fraction of the sinusoidal surface that is subjected to normalized pressure between p_n/\mathbf{s}_Y and $(p_n + dp_n)/\mathbf{s}_Y$. The result is specified by the functional relationship

$$q_n \left(\frac{p}{\mathbf{s}_Y} \right) = q \left(\frac{p}{\mathbf{s}_Y}, \frac{\bar{p}_n}{\mathbf{s}_Y}, \mathbf{y}_n \right) \quad (2)$$

We observe four general regimes of behavior, depending on the normalized contact pressure $\mathbf{x} = \bar{p}/\mathbf{s}_Y$, as outlined in the next sections.

3.1 Elastic Regime $0 < \mathbf{x} < \mathbf{py} \sin^2(\mathbf{p}/10\mathbf{y})$

In the elastic regime, A , Φ and Φ^{mean} are given by the Westergaard solution (Westergaard 1939)

$$A(\mathbf{x}, \mathbf{y}) = \begin{cases} \frac{2}{\mathbf{p}} \sin^{-1} \sqrt{\frac{\mathbf{x}}{\mathbf{py}}}, & \mathbf{x} < \mathbf{py} \\ 1, & \mathbf{x} \geq \mathbf{py} \end{cases} \quad (\text{A3})$$

$$\Phi(\mathbf{h}, \mathbf{x}, \mathbf{y}) = \begin{cases} \frac{2\mathbf{x} \cos(\mathbf{ph})}{\sin^2(\mathbf{p}A/2)} \left\{ \sin^2(\mathbf{p}A/2) - \sin^2(\mathbf{ph}) \right\}^{1/2} & \mathbf{x} < \mathbf{py} \\ \mathbf{x} + \mathbf{py} \cos(2\mathbf{ph}) & \mathbf{x} > \mathbf{py} \end{cases} \quad (\text{A4})$$

$$\Phi^{mean}(\mathbf{x}, \mathbf{y}) = \begin{cases} \frac{\mathbf{px}}{2\sin^{-1}(\sqrt{\mathbf{x}/\mathbf{py}})} & \mathbf{x} \leq \mathbf{py} \\ \mathbf{x} & \mathbf{x} \geq \mathbf{py} \end{cases} \quad (\text{A5})$$

$$q(\mathbf{h}, \mathbf{x}, \mathbf{y}) = \begin{cases} \frac{\mathbf{h}/\mathbf{p}}{\left[\left\{ (\mathbf{py} - \mathbf{x})^2 + \mathbf{h}^2 \right\} \left\{ 2\mathbf{x} \left(\mathbf{py} - \mathbf{x} + \sqrt{(\mathbf{py} - \mathbf{x})^2 + \mathbf{h}^2} \right) - \mathbf{h}^2 \right\} \right]^{1/2}} & \mathbf{h} < 2\sqrt{\mathbf{pyx}} \\ 0 & \mathbf{h} > 2\sqrt{\mathbf{pyx}} \end{cases} \quad (\text{A6})$$

Note that the elastic solution depends only on the normalized nominal pressure $\mathbf{x} = \bar{\mathbf{p}}/\mathbf{s}_y$ and surface property \mathbf{y} , and is independent of g_n/I_n . The critical load $\mathbf{x} = \bar{\mathbf{p}}/\mathbf{s}_y = \mathbf{py}$ corresponds to full contact ($2a/I = 1$). This suggests a second physical interpretation for the parameter \mathbf{y} : a surface with a low value for \mathbf{y} can easily be flattened.

This solution is valid below the elastic limit: Gao *et al* (2005) suggest that a convenient (but approximate) estimate for the yield point is given by the condition $\mathbf{y}a/I < 0.1$, which requires that $\mathbf{x} = \bar{\mathbf{p}}/\mathbf{s}_y < \mathbf{py} \sin^2(\mathbf{p}/10\mathbf{y})$.

3.2 Elastic-Plastic regime $\mathbf{py} \sin^2(\mathbf{p}/10\mathbf{y}) < \mathbf{x} < 2H_0/\mathbf{y}$

The elastic-plastic regime of behavior is observed for applied loads that slightly exceed yield. Under these conditions, the elastic and plastic strains under the indenter are comparable, and exact expressions for A , Φ and Φ^{mean} cannot be found. Detailed numerical results are given in Gao *et al* (2005). For the problem at hand, however, we find that at most a single scale of roughness is in the elastic-plastic regime, so it is not necessary to characterize this regime in detail. Consequently, we have constructed simple functions for A , Φ and Φ^{mean} by using a self-consistent interpolation between the elastic and fully plastic regimes. The interpolation is constructed to predict correctly: (i) the elastic limit, (ii) the critical load to transition to fully plastic behavior; (iii) the contact pressure distribution at the elastic limit; and (iv) the contact

pressure at the fully plastic limit. In addition, we interpolate the contact size between the elastic and fully plastic limits as follows

$$A(\mathbf{x}, \mathbf{y}) = \frac{(\mathbf{x} - \mathbf{x}_p)}{(\mathbf{x}_e - \mathbf{x}_p)} A_e + \frac{(\mathbf{x} - \mathbf{x}_e)^{0.9}}{(\mathbf{x}_p - \mathbf{x}_e)^{0.9}} A_p \quad (\text{A7})$$

where

$$\begin{aligned} \mathbf{x}_e &= \mathbf{p}\mathbf{y} \sin^2\left(\frac{\mathbf{p}}{10\mathbf{y}}\right) & \mathbf{x}_p &= \frac{2H_0}{\mathbf{y}} & H_0 &= 2.8 \\ A_e &= 1/(5\mathbf{y}) & A_p &= 2/\mathbf{y} \end{aligned} \quad (\text{A8})$$

define dimensionless values of the critical nominal pressure at yield; the critical nominal pressure at full plasticity, and the normalized contact widths at yield and the fully plastic limit, respectively. The contact pressure distribution is approximated as

$$\Phi(\mathbf{h}, \mathbf{x}, \mathbf{y}) = \frac{2\mathbf{a}(\mathbf{x}, \mathbf{y})\cos(\mathbf{p}\mathbf{h})}{\sin^2(\mathbf{p}A/2)} \left\{ \sin^2(\mathbf{p}A/2) - \sin^2(\mathbf{p}\mathbf{h}) \right\}^{1/2} + \mathbf{b}(\mathbf{x}, \mathbf{y}) \quad (\text{A9})$$

where the scaling factors \mathbf{a} and \mathbf{b} are introduced to ensure that the contact pressure has the correct average and maximum values. This requires

$$\mathbf{a}(\mathbf{x}, \mathbf{y}) = \frac{(\mathbf{A}\mathbf{x}^{\max} - \mathbf{x})\sin(\mathbf{p}A/2)}{2A - \sin(\mathbf{p}A/2)} \quad \mathbf{b}(\mathbf{x}, \mathbf{y}) = \frac{2\mathbf{x} - \mathbf{x}^{\max}\sin(\mathbf{p}A/2)}{2A - \sin(\mathbf{p}A/2)} \quad (\text{A10})$$

where the maximum contact pressure is interpolated between its values at yield and full plasticity as

$$\mathbf{x}^{\max} = \frac{(A - A_p)}{(A_0 - A_p)} \frac{\mathbf{x}}{A} + \frac{H_0(A - A_0)}{(A_p - A_0)} \quad (\text{A11})$$

where

$$A_0 = \frac{A_e(H_0 - \mathbf{x}_e/A_e) + A_p(\mathbf{x}_e/A_e - 2\sqrt{\mathbf{p}\mathbf{y}\mathbf{x}_e})}{H_0 - 2\sqrt{\mathbf{p}\mathbf{y}\mathbf{x}_e}} \quad (\text{A12})$$

is a constant chosen to ensure that the peak contact pressure has the correct value

$\mathbf{x}^{\max} = 2\sqrt{\mathbf{p}\mathbf{y}\mathbf{x}_e}$ at the elastic limit ($A = A_e, \mathbf{x} = \mathbf{x}_e$). The mean contact pressure follows as

$$\Phi^{\text{mean}}(\mathbf{x}, \mathbf{y}) = \mathbf{x}/A \quad (\text{A13})$$

In addition, the contact pressure distribution function may be computed as

$$q(\mathbf{h}, \mathbf{x}, \mathbf{y}) = \frac{(\mathbf{h} - \mathbf{b}H_0)/\mathbf{p}}{\left[\left\{ \mathbf{w}^2 + (\mathbf{h} - \mathbf{b}H_0)^2 \right\} \left\{ 2\mathbf{a} \left(\mathbf{w} + \sqrt{\mathbf{w}^2 + (\mathbf{h} - \mathbf{b}H_0)^2} \right) - (\mathbf{h} - \mathbf{b}H_0)^2 \right\} \right]^{1/2}} \quad (\text{A14})$$

$$\mathbf{w} = \mathbf{a} \cot^2(\mathbf{p}A/2)$$

3.3 Fully plastic regime – non-interacting asperities $2H_0/\mathbf{y} < \mathbf{x} < 2H_0/3$

In the fully plastic regime, the plastic strains under the indenter greatly exceed the elastic strains, and the stress fields approach the rigid-plastic limit (given e.g. by slip line field solutions). Here, it is necessary to distinguish between two distinct types of behavior. As long as the contact spots are small (numerical results suggest $2a/\mathbf{l} < 0.67$), there is no interaction between neighboring asperity contacts, and A , Π and Φ^{mean} can be estimated from slip-line field solutions (or numerical simulations) for a flat punch indenting a rigid-plastic half-space as

$$\begin{aligned} A(\mathbf{x}) &= \mathbf{x} / H_0 \\ \Phi(x) &= H_0 \quad (|x|/a < 1) \\ \Phi^{mean} &= H_0 \end{aligned} \quad (\text{A15})$$

where $H_0 \approx 2.9$ is the hardness of the material normalized by its tensile yield stress. Numerical simulations and slip-line field solutions show that H_0 varies weakly with g/\mathbf{l} , but this variation is insignificant for our present purposes. Note that in this regime the contact pressure distribution is perfectly uniform, and the solution is independent of \mathbf{y} . Finally, the pressure distribution function follows as

$$q(\mathbf{h}, \mathbf{x}, \mathbf{y}) = A(\mathbf{x}, \mathbf{y}) \mathbf{d}(\mathbf{h} - H_0) \quad (\text{A16})$$

where $\mathbf{d}(x)$ denotes the Dirac delta distribution.

3.4 Fully plastic regime – interacting asperities $2H_0/3 < \mathbf{x}$

When the size of the contact spots becomes comparable to the wavelength, the plastic strain fields associated with neighboring asperities begin to interact. Numerical simulations show that in this regime, the contact pressure distribution remains approximately uniform, but the magnitude of the pressure increases substantially, and in some cases reaches twice the hardness of the material. This behavior has a dramatic influence on the behavior of fine roughness scales.

As in Section 3.2 we have devised approximate analytical approximations to numerical simulations to simplify our calculations. It is simplest to specify the relationships between \mathbf{x} , \mathbf{y} , A and Φ^{mean} parametrically as

$$\Phi^{mean} = H_0 + (H_1(\mathbf{y}) - H_0)(3A - 2)^3 \quad (\text{A17})$$

$$\mathbf{x} = A\Phi^{mean} \quad (\text{A18})$$

where $H_1(\mathbf{y})$ is the limiting value of the normalized contact pressure $p(x)/\mathbf{s}_y$ at full contact. The following function gives an approximate fit to the results shown in Fig. 8 of Gao *et al* (2004)

$$H_1(\mathbf{y}) = 5.8 - 60/(16 + \mathbf{y}^{3/2}) \quad (\text{A19})$$

It is straightforward to solve these equations to determine the functions defined in Eqs (A1). The results involve the solution to a cubic equation, however, and so are too lengthy to be recorded here. Finally, the contact pressure distribution function in the interacting asperity regime has the same form as that given in Eq. (A16).

Appendix B: Numerical simulations of plastic contact of a truncated Weierstrass profile

A central assumption that underlies the Ciavarella *et al* (2000) model is that successive scales of roughness interact only through the requirement that the true contact pressure acting on the n th scale must equal the nominal contact pressure exerted on the $n+1$ th scale, and the deformation fields otherwise fully decouple. Saint Venant's principle can be used to justify this assumption for elastic solids. For materials that deform plastically, however, there is no rigorous basis for this approximation – and indeed there is good reason to believe that there are circumstances where the deformation fields between successive roughness scales do not decouple. We have therefore conducted finite element simulations of elastic-plastic contact between surfaces with two or more scales of roughness, to investigate the validity of this assumption. A few representative results of these simulations will be outlined here.

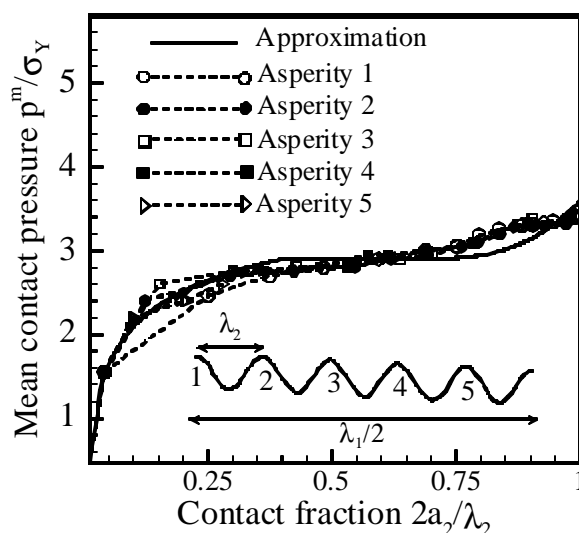


Fig B1: Results of a finite element simulation of the indentation response of an elastic-perfectly plastic solid with two scales of surface roughness. The figure shows the variation of mean pressure with contact fraction for each asperity contact on the finer scale as the load is progressively increased. Our approximation to the behavior of a single roughness scale is shown for comparison.

Fig B1 shows the behavior of an elastic-perfectly plastic solid with two roughness scales, which is indented by a rigid flat indenter. Results are shown for $g = I_1 / I_0 = 10$, $E / s_Y = 200$, $g_0 / I_0 = 1/100$, $g_1 / I_1 = 1/40$ and $n = 0.3$. These parameters correspond to $y_0 = 2$, $y_1 = 5$, and $D = 1.4$. We have computed the mean contact pressure as a function of contact size for each asperity in the finer roughness scale, and compared the results with our approximation to the behavior of a surface with a purely sinusoidal roughness. For small values of $2a_1 / I_1$ the two cases are indistinguishable. For values of $2a_1 / I_1 > 0.6$ (where asperities on the finer scale begin to interact), we find that the pressure on the two-scale surface rises somewhat more gradually than that for a pure sinusoid, but the limiting behavior as $2a_1 / I_1 \rightarrow 1$ is correctly modeled by a single-scale surface.

The results of a second set of simulations are illustrated in Figs B2 and B3. Here, we compare directly the behavior of surfaces with one, two and three scales of roughness, when indented by a rigid flat surface. Results are shown for $g=10$, $E/s_Y=200$, $n=0.3$, $g_0/I_0=1/100$, $g_1/I_1=1/40$, $g_2/I_2=1/16$, which correspond to $D=1.4$, $y_0=2.2$, $y_1=5.5$, $y_2=13.7$. All three scales of roughness are therefore in the fully plastic regime for sufficiently high loads. Fig 15 shows the distribution of contact pressure for the three scales of roughness, for two values of nominal load. These results clearly agree qualitatively with the predictions of our approximate model. In particular, the computations demonstrate the progressive increase in contact fraction and contact pressure on successive scales of roughness, and show also that asperity interactions cause the average contact pressure on scales $n=1$ and 2 to exceed the material hardness.

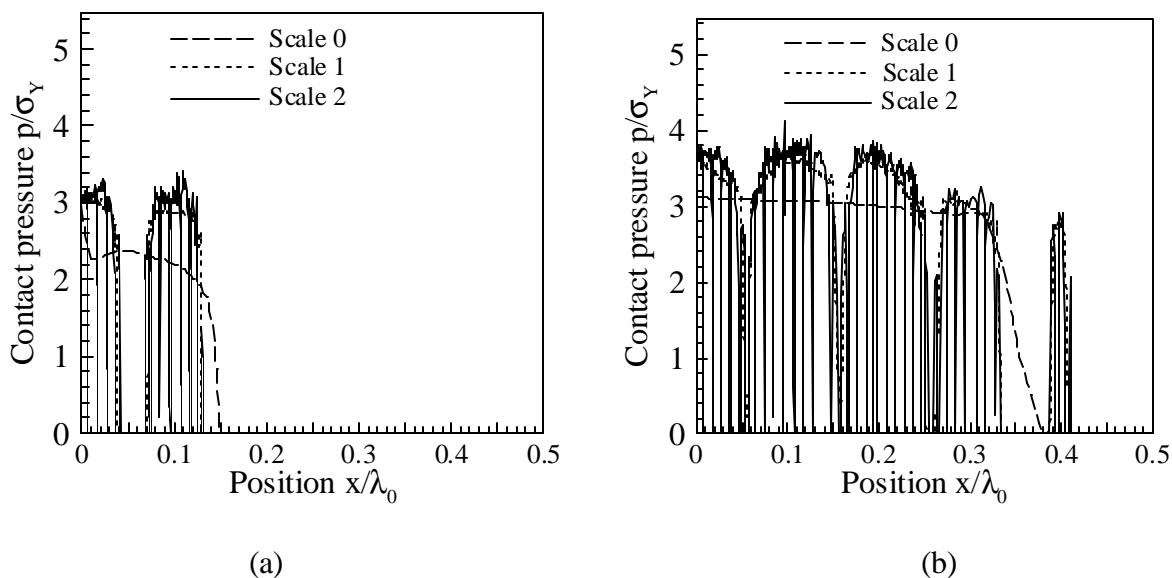


Fig. B2 The contact pressure distribution predicted by finite element computations for truncated Weierstrass surfaces with one, two and three scales of roughness that are indented by a rigid, flat surface. Results are shown for two values of nominal pressure: (a) $p_{-1}/s_Y = 0.624$ (b) $p_{-1}/s_Y = 2.10$

A more quantitative comparison of our numerical and analytical predictions is shown in Fig 16. Here, we have plotted the total true area of contact predicted by finite element computations for each of the three roughness scales, and compared the results with our approximate analytical expression. The analytical results clearly provide a good approximation to the finite element computations.

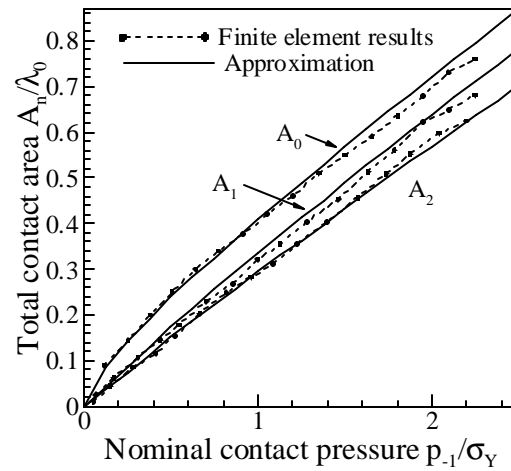


Fig B3: Comparison of the true area of contact predicted by finite element simulations with 1, 2 and 3 scales of roughness with the approximate analytical expressions predicted by assuming each scale behaves as an isolated sinusoid.

Appendix C: Numerical computations of pressure distribution functions.

Elementary calculations show that the pressure distribution function for an elastic-plastic solid will have the form

$$q_n(\mathbf{x}) = \bar{q}_n(\mathbf{x}) + \sum_{j=0}^n Q_j^{(n)} \mathbf{d}(\mathbf{x} - \mathbf{x}_j^{(n)}) \quad (\text{C1})$$

where \bar{q}_n denotes a continuous function, and the sum consists of a series of direct Delta distributions with magnitude $Q_j^{(n)}$, which occur at normalized pressures $\mathbf{x}_j^{(n)}$. Given the n th term in the series, we seek to compute the next term. The general expression is given by

$$q_n(\mathbf{h}) = \int_0^\infty q(\mathbf{h}, \mathbf{x}, \mathbf{y}_n) q_{n-1}(\mathbf{x}) d\mathbf{x} \quad (\text{C2})$$

This integral must be divided into separate contributions that correspond to the elastic regime, elastic plastic regime, and fully plastic regime

$$\begin{aligned} q_n(\mathbf{h}) = & \int_{\mathbf{x}_{\min}^e}^{\mathbf{x}_{\max}^e} q(\mathbf{h}, \mathbf{x}, \mathbf{y}_n) q_{n-1}(\mathbf{x}) d\mathbf{x} + \int_{\mathbf{x}_{\min}^{ep}}^{\mathbf{x}_{\max}^{ep}} q(\mathbf{h}, \mathbf{x}, \mathbf{y}_n) q_{n-1}(\mathbf{x}) d\mathbf{x} \\ & + \int_{\mathbf{x}_{\min}^{fp}}^{\mathbf{x}_{\max}^{fp}} q(\mathbf{h}, \mathbf{x}, \mathbf{y}_n) q_{n-1}(\mathbf{x}) d\mathbf{x} + \int_{\mathbf{x}_{\min}^{fpi}}^{\mathbf{x}_{\max}^{fpi}} q(\mathbf{h}, \mathbf{x}, \mathbf{y}_n) q_{n-1}(\mathbf{x}) d\mathbf{x} \end{aligned} \quad (\text{C3})$$

where the limits are

$$\begin{aligned} \mathbf{x}_{\min}^e &= \mathbf{h}^2 / 4p\mathbf{y}_n & \mathbf{x}_{\max}^e &= \min(\mathbf{x}_{n-1}^{\max}, \mathbf{x}_{n-1}^e) \\ \mathbf{x}_{\min}^{ep} &= \max(p^{\max-1}(\mathbf{h}), \mathbf{x}_{n-1}^e) & \mathbf{x}_{\max}^{ep} &= \min(\mathbf{x}_{n-1}^{\max}, \mathbf{b}^{-1}(\mathbf{h})) \\ \mathbf{x}_{\min}^{fp} &= \max(\mathbf{x}_{n-1}^{\max}, 2H_0/\mathbf{y}_n) & \mathbf{x}_{\max}^{fp} &= \min(\mathbf{x}_{n-1}^{\max}, 2H_0/3) \\ \mathbf{x}_{\min}^{fpi} &= \max(\mathbf{x}_{n-1}^{\max}, 2H_0/3) & \mathbf{x}_{\max}^{fpi} &= \min(\mathbf{x}_{n-1}^{\max}, H_1(\mathbf{y}_n)) \end{aligned} \quad (\text{C4})$$

where \mathbf{x}_n^e denotes the critical value of dimensionless nominal pressure to induce yield in the n th scale; \mathbf{x}_n^{\max} is the maximum dimensionless nominal pressure acting on the n th scale; $p^{\max-1}$ denotes the value of \mathbf{x} that satisfies eq (A11) with $\mathbf{x}^{\max} = \mathbf{h}$; $\mathbf{b}^{-1}(\mathbf{h})$ is the value of \mathbf{x} that satisfies the second of Eq. (A10) with $\mathbf{b} = \mathbf{h}$. Next, recall that that

$$\begin{aligned} q(\mathbf{x}, \mathbf{h}) &= A(\mathbf{x}, \mathbf{y}) \mathbf{d}(\mathbf{h} - H_0) & \mathbf{x}_{\min}^{fp} &< \mathbf{x} < \mathbf{x}_{\max}^{fp} \\ q(\mathbf{x}, \mathbf{h}) &= A(\mathbf{x}, \mathbf{y}) \mathbf{d}(\mathbf{h} - \Phi^{mean}(\mathbf{x})) & \mathbf{x}_{\min}^{fpi} &< \mathbf{x} < \mathbf{x}_{\max}^{fpi} \end{aligned} \quad (\text{C5})$$

Substitute into (C2) to see that

$$\begin{aligned}
q_n(\mathbf{h}) &= \int_{\mathbf{x}_{\min}^e}^{\mathbf{x}_{\max}^e} q(\mathbf{h}, \mathbf{x}, \mathbf{y}_n) \bar{q}_{n-1}(\mathbf{x}) d\mathbf{x} + \int_{\mathbf{x}_{\min}^{ep}}^{\mathbf{x}_{\max}^{ep}} q(\mathbf{h}, \mathbf{x}, \mathbf{y}_n) \bar{q}_{n-1}(\mathbf{x}) d\mathbf{x} + \mathbf{d}(\mathbf{h} - H_0) \int_{\mathbf{x}_{\min}^{fp}}^{\mathbf{x}_{\max}^{fp}} A(\mathbf{x}, \mathbf{y}_n) \bar{q}_{n-1}(\mathbf{x}) d\mathbf{x} \\
&+ \int_{\mathbf{x}_{\min}^{fpi}}^{\mathbf{x}_{\max}^{fpi}} A(\mathbf{x}, \mathbf{y}_n) \mathbf{d}(\mathbf{h} - \Phi^{mean}(\mathbf{x})) \bar{q}_{n-1}(\mathbf{x}) d\mathbf{x} + \sum_{j=0}^{n-1} Q_j^{(n-1)} A(\mathbf{x}_j^{n-1}, \mathbf{y}_n) \mathbf{d}(\mathbf{h} - \Phi^{mean}(\mathbf{x}_j^{n-1}, \mathbf{y}_n))
\end{aligned} \tag{C6}$$

Hence

$$\begin{aligned}
Q_0^n &= \int_{\mathbf{x}_{\min}^{fp}}^{\mathbf{x}_{\max}^{fp}} A_{fp}(\mathbf{x}, \mathbf{y}_n) \bar{q}_{n-1}(\mathbf{x}) d\mathbf{x} \\
Q_j^n &= Q_{j-1}^{(n-1)} A_{fpi}(\mathbf{x}_{j-1}^{(n-1)}, \mathbf{y}_n) \\
\mathbf{x}_j^n &= \Phi^{mean}(\mathbf{x}_{j-1}^{n-1}, \mathbf{y}_n)
\end{aligned} \tag{C7}$$

$$\begin{aligned}
\bar{q}_n(\mathbf{h}) &= \int_{\mathbf{x}_{\min}^e}^{\mathbf{x}_{\max}^e} q(\mathbf{h}, \mathbf{x}, \mathbf{y}_n) \bar{q}_{n-1}(\mathbf{x}) d\mathbf{x} + \int_{\mathbf{x}_{\min}^{ep}}^{\mathbf{x}_{\max}^{ep}} q(\mathbf{h}, \mathbf{x}, \mathbf{y}_n) \bar{q}_{n-1}(\mathbf{x}) d\mathbf{x} \\
&+ \int_{\mathbf{x}_{\min}^{fpi}}^{\mathbf{x}_{\max}^{fpi}} A(\mathbf{x}, \mathbf{y}_n) \mathbf{d}(\mathbf{h} - \Phi^{mean}(\mathbf{x})) \bar{q}_{n-1}(\mathbf{x}) d\mathbf{x}
\end{aligned}$$